2013 European Control Conference (ECC)
July 17-19, 2013, Zürich, Switzerland.

POD-based state estimation of simulated moving bed chromatographic processes

Boulaïd Boulkroune[†], Michel Kinnaert[†] and Ali Zemouche[§]

Abstract— **Chromatographic separation is a powerful technique based on the differential adsorption of the components of a mixture. In simulated moving bed (SMB) chromatographic processes, a counter-current movement of the liquid and the solid phases is achieved by periodically switching the inlet and the outlet ports in a closed loop of chromatographic columns. This paper addresses the problem of state observation of simulated moving bed (SMB) chromatographic processes. The proposed approach is based on a reduced model obtained via the proper orthogonal decomposition (POD) method. The state estimation is performed using a nonlinear observer designed for Lipschitz LPV (linear parameter varying) systems. Numerical simulations are provided to validate the proposed approach.**

I. Introduction

Chromatographic separation is a powerful technique based on the differential adsorption of the components of a mixture. It is widespread in the fine chemicals, biotechnology and pharmaceutical industries for separation, extraction and purification of complex mixtures. Originally, chromatography is a discontinuous process (batch). However, several continuous processes like the simulated moving bed (SMB) process have been developed. SMB processes are characterized by a counter-current movement of the liquid and the solid phase which is achieved by switching periodically the inlet and outlet ports of a closed loop of chromatographic columns.

The problem of designing nonlinear observers has received great attention in literature. This problem is motivated by certain applications such as fault diagnosis and control system design. The challenge in the observer design is to estimate all states of the considered systems asymptotically despite the presence of disturbances, based only on few measurements. In the continuous-time case, various state observation methods for nonlinear Lipschitz systems have been proposed, see for example [1], [2], [3], to name only a few. Other methods dedicated to the discrete-time case are presented in ([4], [5]). Unfortunately all these approaches can not be applied in our case since the SMB model combines a linear parameter varying part and a Lipschitz nonlinearity[a]. Therefore, one of the contributions of this paper is to extend previous works on nonlinear observers to this larger model class.

From the application point of view, the challenge in the design of state observers for SMB processes lies in their description by a set of nonlinear partial differential equations (PDEs). Spatial discretization is usually the first step for observer design, which yields high order models. Therefore, high dimensional observability problems can be encountered. In [6], the authors have developed a linear observer based on a linearized model of the SMB process. The observer gain is computed using an heuristic approach based on physical considerations and simulation trials. A different approach is proposed in [7] based on the stationary regime which results from the periodic behavior of the SMB process. The considered observer is used to determine the form, position and propagation velocity of the fluid concentration profiles. Based on the approximation of the concentration profiles by a weighted sum of some chosen truncated exponential functions, a receding horizon state estimation scheme for SMB process is proposed in [8]. In [9], a state observer for SMB process with nonlinear adsorption isotherms is designed. It is based on a simple Luenberger-like correction term. The observe gains are calculated using the Riccati-like approach. An extended Kalman filter for a true moving bed (TMB) model is proposed in [10] and a Luenberger observer is designed in [11] based on the approximation of the SMB profile by wave forms. The extended Kalman filter is also used in [12] and [13]. Recently, an interesting work based on moving horizon state and parameter estimation for SMB processes has been proposed in [14]. Unfortunately, this approach is computationally demanding since the estimation problem is formulated as an optimization problem and solved based on a real-time scheme.

In the work reported here, a reduced order model obtained by proper orthogonal decomposition (POD) will be used. Contrary to [6], this model retains the nonlinear effects and contrary to [7] it allows to describe the complete concentration profiles. The POD approach, based on empirical data or snapshots, identifies both a useful set of basis functions and the dimension of the subspace necessary to achieve a satisfactory approximation of the system. A reduced order model can be obtained by projecting the dynamics of the original model to this subspace ([15] and [16]). To further reduce the computing load, no on-line computation of the observer gains is performed, as opposed to receding horizon and Kalman-like approaches. The main objective of this work is thus to propose a nonlinear LPV observer achieving state estimation for a SMB process based on POD model.

[†]Department of Control Engineering and System Analysis, Université Libre de Bruxelles (ULB), CP 165/55, 50 Av. F.D. Roosevelt, 1050 Brussels, Belgium (e-mails : Boulaid.Boulkroune@ulb.ac.be and Michel.Kinnaert@ulb.ac.be).

[§]Centre de Recherche en Automatique de Nancy, CNRS-UMR 7039, Nancy-Université, 54400 Cosnes et Romain, France (e-mails : Ali.Zemouche@iut-longwy.uhp-nancy.fr)

[a]By an abuse of language, this model class will be called "nonlinear LPV model" in the paper.

II. SMB PROCESS MODEL

The SMB process is subdivided into four different sections delimited by several material flow outlets and inlets, as illustrated in Fig 1 where separation of a binary mixture of components A and B is considered . The two inlets are the input of the mixture to be separated and the input of a desorbing solvent. The process also contains two withdrawal ports, one for the raffinate which is constituted mostly of the less adsorbable component (component A) and another for the extract which mostly consists of the most retained component (component B). The movement of the liquid and solid phases, as well as the adsorption-desorption phenomena taking place in each section are depicted in figure 1.

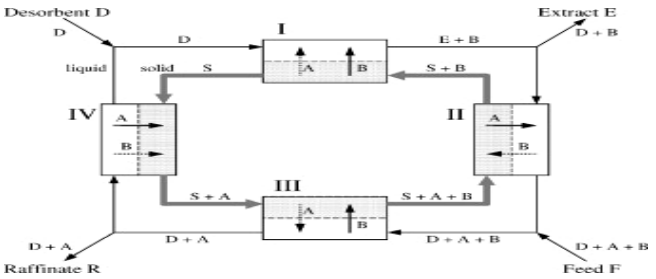

Fig. 1. Equivalent counter-current representation of a simulated moving bed process for separation of a mixture with two species A and B - material fliows and adsorption/desorption phenomena in each section.

In the literature various approaches are proposed to describe the dynamic behavior of the SMB process. They differ in the assumptions used to build the mass balance equations [17]. In this work, the linear driving force (LDF) model is chosen for modelling a SMB plant containing eight columns (2-2-2-2 configuration) and used to separate a binary mixture of components A and B. The following assumptions are made to derive the model equations:

- The columns are assumed to be radially homogeneous;
- Compressibility of the mobile phase is negligible;
- Isothermal operating conditions are considered;
- Only components A and B are adsorbed.

In each column, the mass balance equation in the fluid phase is expressed by :

$$\frac{\partial c_k^i}{\partial t} = D_{k,j}\frac{\partial^2 c_k^i}{\partial z^2} - v_j\frac{\partial c_k^i}{\partial z} - K_\varepsilon\frac{\partial q_k^i}{\partial t}, \quad K_\varepsilon = \frac{1-\varepsilon}{\varepsilon} \quad (1)$$

where c_k^i the fluid concentration; q_k^i the solid concentration; v_j the fluid velocity; ε the porosity; $D_{k,j}$ the diffusivity. t and z are the time and the axial coordinate, respectively. $k = A, B$ refers to the species in the mixture to separate. $j = I, II, III, IV$ refers to each zone of the SMB plant while the upper-index $i = 1, ...N_c$ with $N_c = 8$ indicates the column. Note that since two columns per zone are considered, $j = I$ for $i = 1, 2$, $j = II$ for $i = 3, 4$, $j = III$ for $i = 5, 6$, $j = IV$ for $i = 7, 8$ at process start-up. In this work, it is assumed that the columns are fixed and the inlet and outlet ports move after each switching period τ.

The mass balance equation in the solid phase, in each column, is given by :

$$\frac{\partial q_k^i}{\partial t} = k_k(q_k^{i,eq} - q_k^i) \quad (2)$$

where k_k is the mass transfer coefficient. $q_k^{i,eq}$ is the adsorbed equilibrium concentration which can be related to the liquid concentration by means of a Langmuir isotherm for the considered mixture [18]:

$$q_k^{i,eq} = \frac{a_k c_k^i}{1 + \sum_{k=1}^{2} b_k c_k^i}$$

where a_i and b_i represent, respectively, the Henry coefficients and the adsorption equilibrium constants.

To complete the previous equations, boundary conditions (BC) in the inlet and outlet of each column are required. BC between columns inside a zone are given by: $c_k^{p-1}(L,t) = c_k^p(0,t)$ indicating that, for a given column p, the inlet concentration is taken as the outlet concentration in column $p-1$. L denotes the column length.

At the startup position, the boundary conditions associated to the inlet and outlet ports are the following:

- in the eluent stream : $v_I c_k^1(0,t) = v_{IV} c_k^8(L,t)$;
- in the extract port : $c_k^3(0,t) = c_k^2(L,t)$;
- in the feed inlet : $v_{III} c_k^5(0,t) = v_{II} c_k^4(L,t) + c_k^{Fe} v_{Fe}$;
- in the raffinate port : $c_k^7(0,T) = c_k^6(L,t)$.

In the last point of each column, as proposed in (Haag et al., 2001), a simple advection equation is used :

$$\frac{\partial c_k^i(L,t)}{\partial t} = -v_j\frac{\partial c_k^i(L,t)}{\partial z} \quad (3)$$

The initial conditions are given by : $c_k^i(z,0) = c_{k,0}^i$.

Besides these equations, the operating conditions are specified by the switching time and the flow rates. A method to choose the operating conditions based on the triangle theory is presented in [18]. The relations between the flow rates are obtained by means of mass balances, so that:

$$\begin{aligned} \text{Desorbent node} &: \quad Q_{IV} + Q_{De} = Q_I \\ \text{Extract node} &: \quad Q_I - Q_{Ex} = Q_{II} \\ \text{Feed node} &: \quad Q_{II} + Q_{Fe} = Q_{III} \\ \text{Raffinate node} &: \quad Q_{III} - Q_{Ra} = Q_{IV} \end{aligned}$$

where Q_{I-IV} are the flow rates in the corresponding zones, Q_{De}, Q_{Ex}, Q_{Fe} and Q_{Ra} denote the external flow rates. The relation between flow rates and velocities is expressed by : $Q_j = \varepsilon S v_j$ with $j = I, II, III, IV$ where S is the cross section of the column.

A. Discretization with the Finite Element Method

In order to solve the system of equations (1)-(2) together with their boundary conditions and their initial conditions, the finite element method is chosen. The structure of model (1)-(2) is a special case of the following reaction-diffusion-convection system:

$$x_t = Dx_{zz} - vx_z + f(x) \quad (4a)$$

$$x(t=0,z) = x_0(z) \quad (4b)$$

where $x_t = \frac{\partial x}{\partial t}$, $x_z = \frac{\partial x}{\partial z}$ and $x_{zz} = \frac{\partial^2 x}{\partial z^2}$ with the boundary conditions :

$$Dx_z + qx = g(x) \quad (5)$$

Dirichlet BC, also known as essential BC, are not included in this formulation since they can be approximated using Neumann (or natural) BC (5) by selecting a large transfer coefficient q and setting $g = qx^*$ where x^* is the value of x on the boundary. The reason for employing this approximation is that Neumann BC can be included into the FEM formulation in a natural way. Notice that in our application, Dirichlet and Neumann BC are considered at each column inlet and outlet, respectively.

In the FEM method, the spatial domain is discretized into a number of finite elements. The original model (4a)-(5) with boundary conditions is then approximated by a number of ordinary differential equations. For more details about this method, the reader is referred to the literature ([19], [20] and [21]). Consider the spatial domain divided into N finite discrete elements, the ODE system associated to the PDE given by equations (4a)-(5) can be expressed as:

$$\frac{dX}{dt}=-M_M^{-1}(D.D_M+v.C_M+q.B_M)X+F(X)+M_M^{-1}G$$

where M_M, D_M, C_M and B_M are, respectively, the mass, diffusion, convection and homogenous boundary matrices. X is the discretized version of x over z. F corresponds to the value of discretized version of the nonlinear function f. G is a vector with all elements equal to zero except in the boundary points (in 1D problems these correspond to the first and last points) in which it takes the value of g in Eqns (5). In the same way, matrix B_M is a matrix of zeros except in the boundary (for 1D problems $B_M(1,1)$ and $B_M(N,N)$). The non-zero entries take the value 1 for Robin boundary conditions (BC), 0 for Neuman BC and a large number (e.g. 10^5) for Dirichlet BC.

B. State-Space Representation

In each column of the SMB plant, the ODE approximation of the concentrations cA, cB, qA and qB can be written as follows :

$$\begin{aligned}\frac{dX_{cA}^i}{dt} &= -M_M^{-1}(D_{A,i}.D_M + v_i.C_M + B_M)X_{cA}^i \\ &\quad + F_{cA}^i(X_{cA}^i, X_{cB}^i, X_{qA}^i) + M_M^{-1}G_{cA}^i(X_{cA}, v_{Fe}) \quad (6)\\ \frac{dX_{cB}^i}{dt} &= -M_M^{-1}(D_{B,i}.D_M + v_i.C_M + B_M)X_{cB}^i \\ &\quad + F_{cB}^i(X_{cA}^i, X_{cB}^i, X_{qB}^i) + M_M^{-1}G_{cB}^i(X_{cB}, v_{Fe}) \quad (7)\\ \frac{dX_{qA}^i}{dt} &= F_{qA}^i(X_{cA}^i, X_{cB}^i, X_{qA}^i) \quad (8)\\ \frac{dX_{qB}^i}{dt} &= F_{qB}^i(X_{cA}^i, X_{cB}^i, X_{qB}^i) \quad (9)\end{aligned}$$

where X_{st}^i is the concentration st in column i with $st = cA, cB, qA, qB$ and $X_{st} = \left[\begin{array}{cccc} X_{st}^{1\prime} & X_{st}^{2\prime} & \cdots & X_{st}^{8\prime}\end{array}\right]'$. Each entry of the vector field $F_{st}^i(X_{cA}^i, X_{cB}^i, X_{qA}^i)$ is a nonlinear function of X_{cA}^i, X_{cB}^i and X_{qA}^i that takes the form:

$$F_{cA}^i(\kappa) = -K_\varepsilon^i k_A^i(\frac{a_A X_{cA}^i(\kappa)}{1+b_A X_{cA}^i(\kappa)+b_B X_{cB}^i(\kappa)} - X_{qA}^i(\kappa)) \quad (10)$$

$$F_{cB}^i(\kappa) = -K_\varepsilon^i k_B^i(\frac{a_B X_{cB}^i(\kappa)}{1+b_A X_{cA}^i(\kappa)+b_B X_{cB}^i(\kappa)} - X_{qB}^i(\kappa)) \quad (11)$$

$$F_{qA}^i(\kappa) = k_A^i(\frac{a_A X_{cA}^i(\kappa)}{1+b_A X_{cA}^i(\kappa)+b_B X_{cB}^i(\kappa)} - X_{qA}^i(\kappa)) \quad (12)$$

$$F_{qB}^i(\kappa) = k_B^i(\frac{a_B X_{cB}^i(\kappa)}{1+b_A X_{cA}^i(\kappa)+b_B X_{cB}^i(\kappa)} - X_{qB}^i(\kappa)) \quad (13)$$

for $\kappa = 1, \cdots, N$.

The function G_{st}^i is a vector with all elements equal to zero except the first element. This one is given by $g = qx^*$ where x^* is the value of x on the boundary. As an example, let us take G_{cA}^1 :$G_{cA}^1 = \left[\begin{array}{cccc} B_M(1,1)X_{cA}^8(N) & 0 & \cdots & 0\end{array}\right]'$ where N is the number of finite elements or the number of spatial discretization points in each column.

In the end of each column, the following equations hold :

$$\frac{dX_{sst}^i(N)}{dt} = -v_i.grad(N,:)X_{sst}^i \quad (14)$$

where $sst = cA, cB$ and $grad = M_M^{-1}C_M$ which represents the discretized version of the operator $\frac{\partial}{\partial z}$ in (3). We recall that the notation $\Lambda(N,:)$ indicates the N^{th} line of matrix Λ.

The equations (6)-(14) can be represented together as follows :

$$\begin{aligned}\frac{dX_{cA}^i}{dt} &= \left[\begin{array}{c} -\overline{M_M}(1:N-1,:)(D_{A,i}.D_M + v_i.C_M + B_M) \\ -v_i.grad(N,:)\end{array}\right] X_{cA}^i \\ &\quad + \left[\begin{array}{c} F_{cA}^i(1:N-1,:) \\ 0\end{array}\right] + \overline{M_M}G_{cA}^i(X_{cA}, v_{Fe}) \quad (15)\\ \frac{dX_{cB}^i}{dt} &= \left[\begin{array}{c} -\overline{M_M}(1:N-1,:)(D_{B,i}.D_M + v_i.C_M + B_M) \\ -v_i.grad(N,:)\end{array}\right] X_{cB}^i \\ &\quad + \left[\begin{array}{c} F_{cB}^i(1:N-1,:) \\ 0\end{array}\right] + \overline{M_M}G_{cB}^i(X_{cB}, v_{Fe}) \quad (16)\\ \frac{dX_{qA}^i}{dt} &= F_{qA}^i(X_{cA}^i, X_{cB}^i, X_{qA}^i) \quad (17)\\ \frac{dX_{qB}^i}{dt} &= F_{qB}^i(X_{cA}^i, X_{cB}^i, X_{qB}^i) \quad (18)\end{aligned}$$

with $\overline{M_M} = M_M^{-1}$.

The concentrations of the two substances of the mixture are measured in three positions only : the extract port, the raffinate port, and behind the first column. The first two sensors (in the extract and raffinate) are moved after a period τ and the third sensor is fixed at the end of the first column. Each sensor measures the concentration in component A and the concentration in component B; therefore, it is represented by two components in the output vector y below. The output equation can be written as:

$$y = H^T X \qquad T = 1, 2, \cdots \quad (19)$$

with $X = \left[\begin{array}{cccc} X_{cA}{}' & X_{cB}{}' & X_{qA}{}' & X_{qB}{}'\end{array}\right]$, where T denotes the number of switching periods (multiple of τ).

Before the first switching instant, matrix H^0, can be given as: $H^0 = \left[\begin{array}{c} H_{mov}^0 \\ H_{fix}\end{array}\right]$, where :

$$H_{fix} = \left[\begin{array}{ccccccccc} \overbrace{0 & \cdots & 1}^{N} & & 0 & \cdots & 0 & 0 & \cdots & 0 \\ \underbrace{0 & \cdots & 0}_{8N} & & \underbrace{0 & \cdots & 1}_{N} & & 0 & \cdots & 0\end{array}\right]$$

$H^0_{mov}=$

$$\begin{bmatrix} \overbrace{0\ \cdots\ 0\ 1}^{2N} & 0\ \cdots\ \cdots\ 0 & 0\ \cdots\ \cdots\ 0 \\ \overbrace{0\ \cdots\ 0\ 1}^{6N} & 0\ \cdots\ \cdots\ 0 & 0\ \cdots\ \cdots\ 0 \\ \overbrace{0\ \cdots\ \cdots\ 0}^{8N} & \overbrace{0\ \cdots\ 0\ 1}^{2N} & 0\ \cdots\ \cdots\ 0 \\ \overbrace{0\ \cdots\ \cdots\ 0}^{8N} & \overbrace{0\ \cdots\ 0\ 1}^{6N} & 0\ \cdots\ \cdots\ 0 \end{bmatrix}$$

As already mentioned, we suppose that the columns are fixed and the inlet and outlet ports are moved periodically in the direction of the liquid flow. Letting $\bar{v}_T = \begin{bmatrix} v'_{T,1} & v'_{T,2} & \cdots & v'_{T,N_c} \end{bmatrix}'$ where $v_{T,i}$ denotes the fluid velocity within the i-th column (i.e, $v_{T,i} = \bar{v}_T(i)$), the velocity vector $\bar{v}_T$ at time instant $T+1$ is updated as :

$$\bar{v}_{T+1} = M_v \times \bar{v}_T \tag{20}$$

In (20), M_v is a permutation matrix that shifts the velocity vector at each switching time T and is given by:

$$M_v = \begin{bmatrix} 0 & 1 \\ I_{N_c-1} & 0 \end{bmatrix}$$

Matrix H^{T+1} is computed, in the the same manner, as follows :

$$H^{T+1} = \begin{bmatrix} H^T_{mov} F_h \\ H_{fix} \end{bmatrix} \tag{21}$$

with $F_h = \mathbf{diag}(M_h, M_h, M_h, M_h)$, where $M_h = \begin{bmatrix} 0 & I_N \\ I_{N\times(N_c-1)} & 0 \end{bmatrix}$. $\mathbf{diag}(A_1, \cdots, A_i)$ indicates a block diagonal matrix with the square matrices $A_1, \cdots, A_i$ on the diagonal.

The boundary functions $G^{T+1,i}_{cA}$ and $G^{T+1,i}_{cB}$ have the structure examplified by G^1_{cA} above equation (14). However, the first component changes depending on the activated mode or equivalently on the position of the inlet and outlet ports. By introducing $v_{T,i}$, $G^{T,i}_{cA}$, $G^{T,i}_{cB}$ and H^T into (15) - (19) in order to characterize the cyclic behavior of the process, the following model is obtained:

$$\frac{dX^i_{cA}}{dt} = \begin{bmatrix} -\overline{M_M}(1:N-1,:)(D_{A,i}.D_M v + v_{T,i}C_M + B_M) \\ -v_{T,i} grad(N,:) \end{bmatrix} X^i_{cA} + \begin{bmatrix} F^i_{cA}(1:N-1,:) \\ 0 \end{bmatrix} + \overline{M_M} G^{T,i}_{cA}(X_{cA}, v_{Fe}) \tag{22}$$

$$\frac{dX^i_{cB}}{dt} = \begin{bmatrix} -\overline{M_M}(1:N-1,:)(D_{B,i}.D_M + v_{T,i}C_M + B_M) \\ -v_{T,i} grad(N,:) \end{bmatrix} X^i_{cB} + \begin{bmatrix} F^i_{cB}(1:N-1,:) \\ 0 \end{bmatrix} + \overline{M_M} G^{T,i}_{cB}(X_{cB}, v_{Fe}) \tag{23}$$

$$\frac{dX^i_{qA}}{dt} = F^i_{qA}(X^i_{cA}, X^i_{cB}, X^i_{qA}) \tag{24}$$

$$\frac{dX^i_{qB}}{dt} = F^i_{qB}(X^i_{cA}, X^i_{cB}, X^i_{qB}) \tag{25}$$

$$y = H^T X \tag{26}$$

$$T \leq t \leq (T+1) \tag{27}$$

C. POD-based model order reduction

Proper orthogonal decomposition (POD) is a powerful and elegant method to obtain a low-dimensional approximate description of a high dimensional process. In the SMB application, it consists in approximating the concentration profiles $c^i_A(t,z)$, $c^i_B(t,z)$, $q^i_A(t,z)$, $q^i_B(t,z)$ by truncated series developments whose coefficients become the new state variables. To explain the principle of the approach, let us consider the general system given by equations (4a)-(4b).

The procedure consists in obtaining an orthonormal basis $\phi(z)$ for the axial coordinate z so that the solution of the PDE model given by equations (4a)-(4b) can be approximated as a truncated series of the form :

$$x(z,t) = \sum_{k=1}^{P} m_k(t)\phi_k(z) \tag{28}$$

where $m_j(t)$ are the modal coefficients that collect the time evolution of the field x. P represents the retained POD modes. The spatially dependent functions $\phi_j(z)$ (eigenfunctions) are the solution of the eigenvalue problem (29) below. In the POD technique, the set of basis functions are computed as those which minimize the distance between the solution of PDE equation computed around different operating points (snapshots) and the subspace built with such basis. The solution of this optimization leads to the following eigenvalue problem:

$$\phi_j(z) = \lambda_j \int_\Omega \mathcal{K}(z,w)\phi_j(w)dw \tag{29}$$

with $\int_\Omega \phi_i(z)'\phi_j(z)dz = \begin{cases} 1 & \text{if } i=j \\ 0 & \text{otherwise} \end{cases}$

where $\Omega = [0; L]$. The eigenvalues λ_j will be arranged so that $\mid \lambda_i \mid \geq \mid \lambda_j \mid$ for $i < j$. $\mathcal{K}(z,z') \in R^{N\times N}$ represents a two points correlation kernel obtained from simulations.

As in practice it is impossible to take measurements in an infinite number of spatial points, the discrete version of $\mathcal{K}(z,z')$ will be employed. It is constructed as ([22] and [16]):

$$\mathcal{K} = \frac{1}{k}\sum_{j=1}^{k} \chi^j \chi^{j'} \tag{30}$$

where $\chi^j \in R^N$ are measurements of the original state variable $x(z,t)$ at a finite number N of spatial points and at a specific time t.

The solution of problem (29) can be numerically computed (approximated) by using the FEM matrix M_M as follows:

$$\phi_j = \lambda_j \mathcal{K} M_M \phi_j \tag{31}$$

with $\mathcal{K}$ constructed as in Eqn (30). More details about the approximation of the eigenproblem (29) are given in [23]. It is important to point out that the set of eigenvectors contains the spatial information of the solution (28). Notice that the approximation is carried out by selecting the most energetic basis functions based on the captured energy :

$$E(\%) = 100 \times \frac{\sum_{j=1}^{p} \lambda_j}{\sum_{j=1}^{N} \lambda_j} \tag{32}$$

Now we can apply this procedure to each concentration ($st = cA, cB, qA, qB$) in each column. In order to be able, to reconstruct the solution, the modes m^i_{st} (time information), with $i = 1, \cdots, N_c$ and $st = cA, cB, qA, qB$, have to be computed. For that purpose, let us define the spatial projection operator as $P^i_{st} = {\Phi^i_{st}}' M_M$, where Φ^i_{st} represents the eigenfunctions for the concentration st in column i.

Applying this operator to (22)-(26) the following equations are obtained:

$$\frac{dm^i_{cA}}{dt} = \rho^i_{cA}(v_{T,i})m^i_{cA} + P^i_{cA}\begin{bmatrix} F^i_{cA}(1:N-1,:) \\ 0 \end{bmatrix} + {\Phi^i_{cA}}' G^{T,i}_{cA}(\Phi_{cA}m_{cA}, v_{Fe}) \quad (33)$$

$$\frac{dm^i_{cB}}{dt} = \rho^i_{cB}(v_{T,i})m^i_{cB} + P^i_{cB}\begin{bmatrix} F^i_{cB}(1:N-1,:) \\ 0 \end{bmatrix} + {\Phi^i_{cB}}' G^{T,i}_{cB}(\Phi_{cB}m_{cB}, v_{Fe}) \quad (34)$$

$$\frac{dm^i_{qA}}{dt} = P^i_{qA}F^i_{qA}(\Phi^i_{cA}m^i_{cA}, \Phi^i_{cB}m^i_{cB}, \Phi^i_{qA}m^i_{qA}) \quad (35)$$

$$\frac{dm^i_{qB}}{dt} = P^i_{qB}F^i_{qB}(\Phi^i_{cA}m^i_{cA}, \Phi^i_{cB}m^i_{cB}, \Phi^i_{qB}m^i_{qB}) \quad (36)$$

where

$$\rho^i_{cA}(v_{T,i}) = P^i_{cA}\begin{bmatrix} -\overline{M_M}(1:N-1,:)(D_{A,i}.D_M + v_{T,i}C_M + B_M) \\ -v_{T,i}grad(N,:) \end{bmatrix}\Phi^i_{cA}$$

$$\rho^i_{cB}(v_{T,i}) = P^i_{cB}\begin{bmatrix} -\overline{M_M}(1:N-1,:)(D_{B,i}.D_M + v_{T,i}C_M + B_M) \\ -v_{T,i}grad(N,:) \end{bmatrix}\Phi^i_{cB}$$

and

$$y = H^T \mathbf{diag}(\Phi_{cA}, \Phi_{cB}, \Phi_{qA}, \Phi_{qB})m \quad (37)$$

with $m = \begin{bmatrix} m'_{cA} & m'_{cB} & m'_{qA} & m'_{qB} \end{bmatrix}'$, $\Phi_{st} = \mathbf{diag}(\Phi^1_{st}, \Phi^2_{st}, \cdots, \Phi^{N_c}_{st})$, $m_{st} = \begin{bmatrix} {m^1_{st}}' & {m^2_{st}}' & \cdots & {m^{N_c}_{st}}' \end{bmatrix}'$ and $T \le t \le T+1$.

Notice that the state variable X^i_{st} can be reconstructed using :

$$X^i_{st}(t) = \Phi^i_{st}m^i_{st}(t). \quad (38)$$

III. Observer design for Lipschitz nonlinear LPV systems

We shall focus on the observer design problem in this section. It will be shown that the previous POD model can be written in a LPV form given by (39a)-(39b) below. Based on this model, a nonlinear LPV observer will be designed such that its state estimation error asymptotically tends to zero.

Let us consider the class of nonlinear systems described by the following equations :

$$\dot{m}(t) = A_{\delta(t)}m(t) + f_{\delta(t)}(m,u) \quad (39a)$$

$$y(t) = C_{\delta(t)}m(t) \quad (39b)$$

where

$$A_{\delta(t)} = \sum_{j=1}^{j=n_\delta} \delta_j(t)A^j, C_{\delta(t)} = \sum_{j=1}^{j=n_\delta} \delta_j(t)C^j$$

$$f_{\delta(t)}(m,u) = \sum_{j=1}^{j=n_\delta} \delta_j(t)f^j(m,u),$$

and $m(t)$ represents the state vector, $u(t)$ is the input vector and $y(t)$ denotes the measured system output. The matrices A^j and C^j for $j = 1, \cdots, n_\delta$ are constant with adequate dimensions. The weighting functions δ_j are assumed known and depend on measurable variables. They verify

$$\sum_{j=1}^{n_\delta} \delta_j(t) = 1,\ 0 \le \delta_j \le 1,\ \forall j \in \{1, \cdots, n_\delta\} \quad (40a)$$

Each nonlinearity $f^j(m,u)$ is assumed to be Lipschitz in m with a known Lipschitz constant γ^j, i.e. $\|f^j(m,u) - f^j(\hat{m},u)\| \le \gamma^j\|m - \hat{m}\|$, $\forall m, \hat{m}$.

The system (33)-(37) can be easily put in the form of system (39a)-(39b) by an appropriate choice of δ_j, since the switching period τ is known. Indeed, the cyclic behaviour of the considered SMB process can be separated into 8 modes corresponding to the 8 possible positions of the input and output ports, each mode lasting for a time period of duration τ. Model (39a)-(39b) can be defined in such a way that mode i corresponds to $\delta_i = 1$ and $\delta_j = 0$ for all $j \ne i$.

The following nonlinear LPV observer is proposed to estimate the state trajectory m :

$$\dot{\hat{m}}(t) = A_{\delta(t)}\hat{m}(t) + f_{\delta(t)}(\hat{m},u) + K_{\delta(t)}(y - C_{\delta(t)}\hat{m}(t)) \quad (41)$$

$$\hat{y}(t) = C_{\delta(t)}\hat{m}(t) \quad (42)$$

with $K_{\delta(t)} = \sum_{j=1}^{j=n_\delta} \delta_j(t)K^j$.

Notice that the only unknown parameter in the observer model is the gain matrix $K_{\delta(t)}$. Thus, the problem amounts to finding this matrix while ensuring the asymptotic convergence of $\hat{m}$ to m. By defining the estimation error $\tilde{m} = m - \hat{m}$, its dynamics can be written as :

$$\dot{\tilde{m}} = \left(A_{\delta(t)} - K_{\delta(t)}C_{\delta(t)}\right)\tilde{m} + \tilde{f}_{\delta(t)}$$

with $\tilde{f}_{\delta(t)} = f_{\delta(t)}(m,u) - f_{\delta(t)}(\hat{m},u)$.

The following theorem gives sufficient conditions for the existence of matrices $K_{\delta(t)}$ that guarantee asymptotic convergence.

Theorem 1: The observation error $\tilde{m}(t)$ converges asymptotically towards zero if there exists matrices R^{j_1}, with $j_1 = 1, \cdots, n_\delta$, a positive definite symmetric matrix P and a positive scalar $\bar{\tau}$ such that the following LMIs are satisfied

$$P > 0 \quad \text{and} \quad \begin{bmatrix} \Psi_{j_1,j_2} & P \\ P & -\bar{\tau}I \end{bmatrix} < 0 \quad (43)$$

$\forall j_1,\ j_2 = 1, \cdots, n_\delta$ where

$$\Psi_{j_1,j_2} = (A^{j_1})'P + PA^{j_1} - (C^{j_2})'(R^{j_1})' - R^{j_1}C^{j_2} + \bar{\tau}(\gamma^{j_1})^2 I \quad (44)$$

Solving LMIs (43) amounts to determining matrices P and R^{j_1}. The matrices K^{j_1}, with $j_1 = 1, \cdots, n_\delta$, can be obtained from $K^{j_1} = P^{-1}R^{j_1}$. ■

Proof: The Lyapunov function candidate for observer design is defined as $\Upsilon = \tilde{m}'P\tilde{m}$, where P is a symmetric positive definite matrix ($P > 0$). Then its derivative is :

$$\dot{\Upsilon} = \tilde{m}'\left[\left(A_{\delta(t)} - K_{\delta(t)}C_{\delta(t)}\right)'P + P\left(A_{\delta(t)} - K_{\delta(t)}C_{\delta(t)}\right)\right]\tilde{m} + \tilde{m}'P\tilde{f}_{\delta(t)} + \tilde{f}'_{\delta(t)}P\tilde{m} \quad (45)$$

By substituting $A_{\delta(t)}$, $C_{\delta(t)}$, $K_{\delta(t)}$ and $\tilde{f}_{\delta(t)}$ by their expressions, we have

$$\dot{\Upsilon} = \sum_{j_1=1}^{n_\delta}\sum_{j_2=1}^{n_\delta} \delta_{j_1}\delta_{j_2}\{\tilde{m}'\left[\left(A^{j_1} - K^{j_1}C^{j_2}\right)'P + P\left(A^{j_1} - K^{j_1}C^{j_2}\right)\right]\tilde{m} + \tilde{m}'P\tilde{f}^{j_1} + (\tilde{f}^{j_1})'P\tilde{m}\} \quad (46)$$

with $j_1,\ j_2 = 1, \cdots, n_\delta$.

Based on the Lipschitz property of each f^{j_1}, one can obtain : $(\gamma^{j_1})^2\tilde{m}'\tilde{m} - (\tilde{f}^{j_1})'\tilde{f}^{j_1} \ge 0$. Then, for any positive constant $\bar{\tau}$, the Lyapunov function derivative can be

expressed as

$$\begin{aligned}\dot{\Upsilon} \leq \dot{\Upsilon} + \sum_{j_1=1}^{n_\delta} \bar{\tau}(\gamma^{j_1})^2 \tilde{m}'\tilde{m} - \bar{\tau}(\tilde{f}^{j_1})'\tilde{f}^{j_1} \\ = \sum_{j_1=1}^{n_\delta}\sum_{j_2=1}^{n_\delta} \delta_{j_1}\delta_{j_2}\{\tilde{m}'\Big[\big(A^{j_1}-K^{j_1}C^{j_2}\big)'P+P\left(A^{j_1}-K^{j_1}C^{j_2}\right)\Big]\tilde{m} \\ + \tilde{m}'P\tilde{f}^{j_1} + (\tilde{f}^{j_1})'P\tilde{m} + \bar{\tau}(\gamma^{j_1})^2\tilde{m}'\tilde{m} - \bar{\tau}(\tilde{f}^{j_1})'\tilde{f}^{j_1}\} \end{aligned} \quad (47)$$

and therefore

$$\dot{\Upsilon} \leq \sum_{j_1=1}^{n_\delta}\sum_{j_2=1}^{n_\delta} \delta_{j_1}\delta_{j_2} \begin{bmatrix}\tilde{m}\\ \tilde{f}^{j_1}\end{bmatrix}' \begin{bmatrix}\overline{\Psi}_{j_1,j_2} & P\\ P & -\bar{\tau}I\end{bmatrix}\begin{bmatrix}\tilde{m}\\ \tilde{f}^{j_1}\end{bmatrix} \quad (48)$$

with

$$\overline{\Psi}_{j_1,j_2} = (A^{j_1})'P + PA^{j_1} - (C^{j_2})'(K^{j_1})'P - PK^{j_1}C^{j_2} + \bar{\tau}(\gamma^{j_1})^2 I$$

By setting $R^{j_1} = P(K^{j_1})$, we have $\dot{\Upsilon} < 0$ if

$$\begin{bmatrix}\Psi_{j_1,j_2} & P\\ P & -\bar{\tau}I\end{bmatrix} < 0 \quad (49)$$

since each $\delta_{j_1},\ \delta_{j_2} \geq 0$, with $j_1, j_2 = 1, \cdots, n_\delta$. Ψ_{j_1,j_2} is defined by (44). The sufficient conditions for the existence of the gain matrices K^{j_1} is based on the existence of a positive constant $\bar{\tau}$ and a positive definite matrix P such that the LMIs (49) hold. Once the solution is obtained, the gain matrices can be determined by $K^{j_1} = P^{-1}R^{j_1}$. □

IV. Simulation results

Fixed working conditions are considered (constant injected concentrations, constant flow rates and constant switching time) and the observer is fed with data corresponding to the cyclic steady state operation. The process parameters used in this work are presented in Table I. The operating conditions are chosen as : $c_A^{Fe} = c_B^{Fe} = 0.5$ vol%, $Q_{Fe} = 0.13159cm^3s^{-1}$, $Q_{Ra} = 0.13631cm^3s^{-1}$, $Q_{Ex} = 0.32969cm^3s^{-1}$ and $Q_1 = 0.10568cm^3s^{-1}$. For obtaining reliable simulation results, it is important to choose the value of N (number of discretization points) properly. To do this, the state space model (22)-(25) is simulated with different values of N. As in [16], a FEM scheme with $N = 71$ per column provides a good approximation of this model. Note that $N = 71$, with eight columns and two components in both liquid and solid phases, implies solving more than 2000 differential equations which makes this scheme computationally demanding for diagnosis and observation purposes. As we discussed before, an alternative consists in reducing the order of the FEM model using the POD method. In this work, A POD−reduced order model (ROM) with $p(X_{cA}, X_{cB}, X_{qA}, X_{qB})^{\text{b}} = 10/10/10/10$ is chosen for representing the FEM model since it gives an accurate result compared to other ROMs. This POD model is validated at several operating points in the neighborhood of the nominal operating point. Besides, it is important to note that the computation time of the obtained POD model is drastically reduced with respect to the computation time of the FEM model. As an example, for a simulation running from $t = 0$min to $t = 600$min, the computation times of the FEM model and the POD model are 52.41min and 11.99min, respectively.

TABLE I

Model parameters

Number of components	2
Column length	L=25cm
Column radius	R=1cm
Number of theoretical plates	$N_p = 50$
Column diffusivity	$v_j \frac{L}{N_p} cm^2 s^{-1}$
Column distribution	2/2/2/2
Mass transfer coefficient	$k_A = 0.5s^{-1},\ k_B = 0.5s^{-1}$
Total porosity	$\varepsilon = 0.83$
Henry's constants	a_A=5.97,a_B=8.52
adsorption equilibrium constant	$b_A = 0.154l/g,\ b_B = 0.295l/g$
Switching time	$\tau = 180$s

For the observer application presented in this work, the SMB process with constant flows is considered. The gains K^j, with $j = 1, \cdots, 8$ are obtained by solving the LMIs (43) using YALMIP, a toolbox for modeling and optimization in Matlab®. The observer initial conditions are chosen arbitrarily. The convergence of the observer described above is illustrated in figures 2 where the evolution of the spatial profiles of component A (blue) and B (red) at, respectively, the end of the 1^{st} and 7^{th} cycle is presented. We recall that one cycle is complete after 8 switching periods. It can be seen that the observer states reach the real state within 7 switching periods. Also, the rapid convergence of the observer for raffinate and extract concentrations in components A and B is observed in figures 3-4.

V. Conclusion

A state observer able to estimate the complete concentration profiles within a SMB process from three concentration sensors has been developed. It is based on a two step procedure. The first step consists in the determination of a reduced order model that reproduces the process behavior in an operating region of interest. Next a nonlinear state observer with guaranteed convergence is developed for the resulting nonlinear model. Simulation results show the effectiveness of the procedure for model reduction and for observer design.

VI. Acknowledgments

This work is supported by FNRS grant through the FRFC project 2.4.643.08.F. It presents research results of the Belgian Network DYSCO, funded by the interuniversity Attraction Poles Program, initiated by the Belgian State, Science Policy Office.

References

[1] R. Rajamani. Observer for lipschitz nonlinear systems. *IEEE Transactions on Automatic Control*, 43:397–401, 1998.

[2] F. Zhu and Z. Han. A note on observers for lipschitz nonlinear systems. *IEEE Transactions on Automatic Control*, 47:1751–1754, 2002.

[3] A. Alessandri. Design of observers for lipschitz nonlinear systems using lmi. In *IFAC Symposium on Nonlinear Control Systems (NOLCOS04)*, Stuttgart, Germany, 2004.

[4] A. Zemouche and M. Boutayeb. Observer design for lipschitz nonlinear systems. the discrete-time case. *IEEE Transactions on Circuits and Systems II Analog and Digital Signal Processing*, 53(8):777–781, 2006.

[b]This notation is used for indicating the number of equations per column.

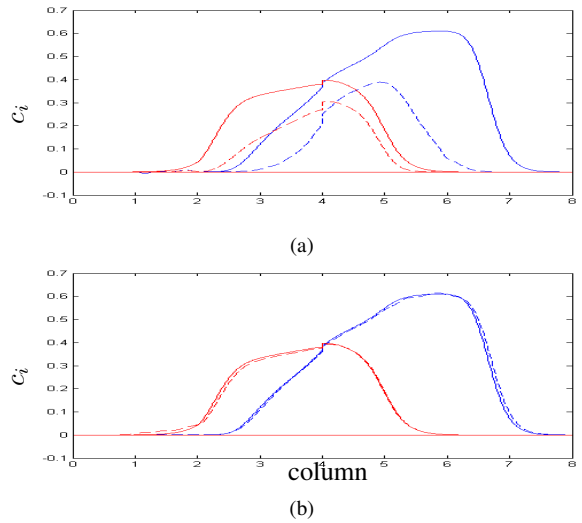

Fig. 2. Spatial profiles of component A (blue) and B (red) in the SMB at the end of the 1st cycle (a) and the 7th cycle (b). Continuous line (real steady-states), dashed line (estimated states).

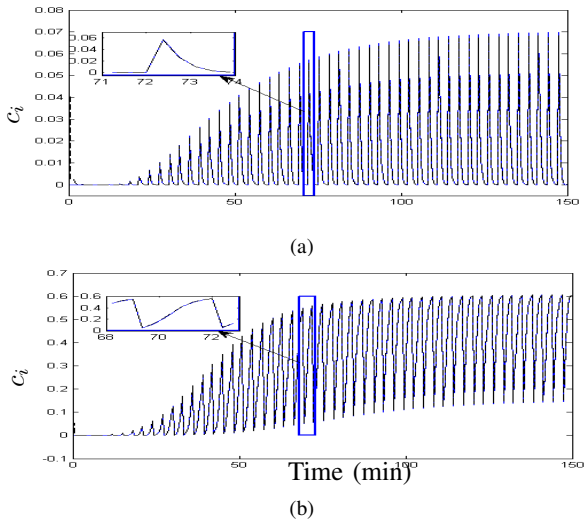

Fig. 3. Convergence of the observer for the point located at the raffinate outlet (a) at the extract outlet (b) for component A. Continuous line (real state), dashed line (estimated state).

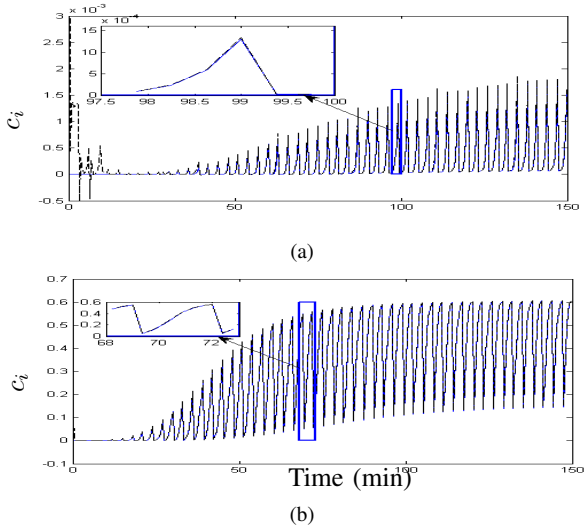

Fig. 4. Convergence of the observer for the point located at the raffinate outlet (a) and at the extract outlet (b) for component B. Continuous line (real state), dashed line (estimated state).

[5] B. Boulkroune, M. Darouach, M. Zasadzinski, S. Gillé, and D. Fiorelli. A nonlinear observer design for an activated sludge wastewater treatment process. *Journal of Process Control*, 19(9):1558 – 1565, 2009.

[6] G. Lauschke, J. Schaffner, M.Zeitz, M. Mangold, and E. D. Gilles. State and parameter estimation for adsorption columns by nonlinear distributed parameter state observers. *Journal of Process Control*, 4(3):163–172, 1994.

[7] J. Lunze and T. Kleinert. Modelling And State Observation Of Simulated Moving Bed Processes. *European Control Conference (ECC)*, Cambridge, UK, 2003.

[8] M. Alamir and J. P. Corriou. Nonlinear receding-horizon state estimation for dispersive adsorption columns with nonlinear isotherm. *Journal of Process Control*, 13, 2003.

[9] J. P. Corriou and M. Alamir. A hybrid nonlinear state observer for concentration profiles reconstruction in nonlinear simulated moving bed. *Journal of Process Control*, 16(4):345–353, 2006.

[10] E. Kloppenburg and E.D. Gilles. Automatic control of the simulated moving bed process for c8 aromatics separation using asymptotically exact input/output-linearization. *Journal of Process Control*, 9(1):41–50, 1999.

[11] T. Kleinert and J. Lunze. Modelling and state observation of Simulated Moving Bed processes based on an explicit functional wave form description. *Mathematics and Computers in Simulation*, 68(1):235–270, 2005.

[12] G. Erdem, S. Abel, M. Morari, M. Mazzotti, M. Morbidelli, and J. H. Lee. Automatic control of simulated moving beds. *Industrial and Engineering Chemistry Research*, 43(2):405–421, 2004.

[13] A. Kupper and S. Engell. Parameter and State Estimation in Chromatographic SMB Processes with Individual Columns and Nonlinear Adsorption Isotherms. *Proc. IFAC, International Symposium of Advanced Control of Chemical Processes (ADCHEM)*, Gramado, Brazil, 611–616, 2006.

[14] A. Küpper, M. Diehl, J.P. Schlöder, H.G Bock, and S. Engell. Efficient moving horizon state and parameter estimation for smb processes. *Journal of Process Control*, 19(5):785–802, 2009.

[15] K. Kunisch and S. Volkwein. Galerkin proper orthogonal decomposition methods for parabolic problems. *Numerische Mathematik*, 99:117–148, 2001.

[16] C. Vilas, and A. Vande Wouwer. Combination of Multi-Model Predictive Control and the Wave Theory for the Control of Simulated Moving Bed Plants. *Chemical Engineering Science*, 66:632–641, 2011.

[17] G. Guiochon, D.G. Shirazi, A. Felinger, and A.M. Katti. Fundamentals of Preparative And Nonlinear Chromatography. *Academic Press, New York*, 1994.

[18] M. Mazzotti, G. Storti, and M. Morbidelli. Optimal operation of simulated moving bed units for nonlinear chromatographic separations. *Journal of Chromatography A*, 769(1):3–24, 1997.

[19] J. N. Reddy. An Introduction to the Finite Element Method. *McGraw-Hill, 2nd edition*, 1993.

[20] O. Zienkiewicz, and K. Morgan. Finite elements and approximation. *John Wiley and Sons*, 1983.

[21] C. Pozrikidis. Introduction to Finite and Spectral Element Methods using Matlab. *Chapman & Hall/CRC*, 2005.

[22] L. Sirovich. Turbulence and the dynamics of coherent structures. I-Coherent structures. *Quarterly of Applied Mathematics*, 45:561–571, 1987.

[23] M.R. García, C. Vilas, J.R. Banga, and A.A. Alonso. Optimal Field Reconstruction of Distributed Process Systems from Partial Measurements. *Industrial & Engineering Chemistry Research*, 46:530–539, 2007.